Energetics Analysis of a Multilevel Global Spectral Model. Part II: Zonal and Meridional Gravitational Energy

SHUN DER KO* AND JOSEPH J. TRIBBIA

*National Center for Atmospheric Research,** Boulder, Colorado*

JOHN P. BOYD

Department of Atmospheric, Oceanic, and Space Science, The University of Michigan, Ann Arbor, Michigan

(Manuscript received 10 October 1988, in final form 27 February 1989)

ABSTRACT

A new approach to energetics is introduced and applied to the NCAR Community Climate Model. All the energy components are separated into gravitational and rotational parts. The new feature of our scheme is that the gravitational divergent kinetic energy is further decoupled into zonal and meridional components, which measure the strength of the east–west and meridional circulations, respectively. The zonal and meridional nondivergent kinetic energies represent the vorticities related to the nondivergent zonal and meridional winds, respectively. The distributions of energy among meridional indices, vertical modes, and zonal waves are analyzed.

We suggest a new, easy, and reasonable criterion to adjust the gravity waves in the initialization based on the vertical modes, meridional indices, and zonal wavenumbers. To retain the strength of large-scale circulations and to preserve the intensity of synoptic scale pressure systems, we recommend that the gravity waves corresponding to the internal modes 2–6, meridional indices 1–6, and zonal wavenumbers 1–10 not be adjusted significantly during the initialization. However, all the other gravity waves can be adjusted initially, particularly those associated with the external and the first internal modes.

1. Introduction

The mass and wind fields obtained from an objective analysis are not necessarily dynamically consistent with a prediction model. Thus unrealistic high-frequency oscillations may result from model integrations when the analyzed data are used directly as an initial state of the model. To adjust these high-frequency gravity waves and thus to generate a balanced initial state for a forecast model, a process known as initialization is often required. Although the nonlinear normal-mode initialization (NNMI) (Baer 1977; Machenhauer 1977) is successful in suppressing the high-frequency gravity waves, the large-scale tropical circulations, such as Hadley and Walker circulations, may be substantially suppressed by the NNMI scheme (Puri and Bourke 1982).

Recently, attempts have been made to incorporate diabatic effects with NNMI. Puri and Bourke (1982) proposed a modified NNMI scheme which retains the Hadley circulation. In this scheme, the gravity waves related to the first internal modes are fully adjusted initially, while for the higher vertical modes, only the horizontal modes with frequencies higher than the cutoff low-frequency are adjusted initially. The cutoff low-frequency is defined as the lowest frequency corresponding to the first internal mode for each zonal wavenumber. But this is not the only way to define a cutoff frequency. Kitade (1983) further incorporated a complete physical parameterization scheme into NNMI. By a modified iteration scheme obtained from Machenhauer's scheme, gravity waves associated with five vertical modes with periods smaller than 48 hours are adjusted initially. With this modified diabatic initialization, the Hadley circulation is well preserved. However, the spinup time started with the initialized data is still much larger than that started with the uninitialized analyzed data.

The aforementioned studies suggest that gravity waves, especially those with low frequencies, play an important role in maintaining the divergence fields, particularly in the tropics. This, however, does not explain how these gravity waves contribute to the large-scale circulations, which include both zonal and meridional circulations. It is important to acquire a more detailed understanding of the behavior of gravity waves in a forecast model. Without this knowledge, additional

---

* Present affiliation: Department of Mathematics and Computer Science, Clarkson University.

** The National Center for Atmospheric Research is sponsored by the National Science Foundation.

Corresponding author address: Dr. Shun Der Ko, Dept. of Mathematics and Computer Science, Clarkson University, Potsdam, N.Y. 13676.

errors could be introduced during the initialization process and thus cause the forecast to drift away from reality.

With observed data, Burrows (1976) investigated the tendency of the kinetic energy of the divergent and nondivergent wind spectra corresponding to zonal wavenumbers 0–24. Chen and Wiin-Nielsen (1976) analyzed the energy budget by using simulated historical data obtained from the second-generation general circulation model developed at the National Center for Atmospheric Research (NCAR). They paid attention mainly to the conversion between total potential energy and the kinetic energy of divergent and nondivergent flow. Kasahara and Puri (1981) employed spectral vertical structure in expanding three-dimensional global data in normal mode functions. Nevertheless, they concentrated primarily on the spectral distribution of total kinetic energy among vertical modes, zonal wavenumbers, and meridional modes. However, these studies did not pay attention to the energy spectra of the divergent and nondivergent kinetic energy for *rotational* and *gravitational* modes.

Note that the gravitational component of the divergent kinetic energy not only plays a major role in the divergence field but also provides necessary information for the initialization, which tends to reduce unrealistic high-frequency oscillations. Furthermore, the nondivergent kinetic energy represents the strength of vorticity that is important to the synoptic scale pressure systems. In addition, the rotational kinetic energy plays an essential role in the Rossby waves, which are the most important elements in the atmospheric motions.

One major intention in this study is to explore *how gravity waves contribute to the zonal and meridional circulations.* Thus, the divergent kinetic energy will be split into zonal and meridional components which measure the strengths of the zonal and meridional circulations, respectively (see section 3). The other purpose of this research is to examine *how gravity waves contribute to the vorticity,* which is important in maintaining the synoptic scale pressure systems. To attain this goal, we shall examine zonal and meridional components of gravitational nondivergent kinetic energy. In order to identify which gravity waves can retain the zonal and meridional circulations and preserve the synoptic scale pressure systems, the distributions of zonal and meridional energies among different frequencies, vertical modes, and zonal waves will be analyzed. Note that our approach is new and different from the previous energetics analysis.

The main procedure for this study is illustrated in Fig. 1. Clearly, the total energy is decomposable into rotational and gravitational energies that consist of divergent and nondivergent kinetic energy and available potential energy (section 2). The gravitational energy includes westward and eastward gravitational energy. The divergent and nondivergent kinetic energy is further split into zonal and meridional components that

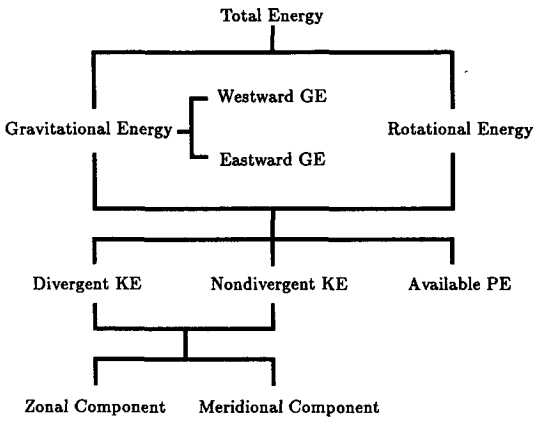

GE: Gravitational Energy

KE: Kinetic Energy

PE: Potential Energy

FIG. 1. Procedures for energetics analysis.

are formulated in section 3. The numerical results are discussed in section 4, and the concluding remarks follow in section 5.

2. Energy in terms of rotational and gravitational modes

We can express the streamfunction ψ, velocity potential χ, and equivalent geopotential $\tilde{\phi}$ as the sum of the vertical and horizontal modes

$$\Lambda(\lambda, \mu, \sigma, t) = \begin{pmatrix} \psi \\ \chi \\ \tilde{\phi} \end{pmatrix} = \sum_J \alpha_J(t) \hat{H}_J(\lambda, \mu) Z_l(\sigma), \quad (1)$$

where

$$\alpha_J = \langle \Lambda \cdot \hat{\Lambda}_J \rangle. \quad (2)$$

Here a dot indicates the inner product defined in Part I (Ko et al. 1989), λ is longitude, μ the sine of latitude, σ the vertical sigma coordinate, and t is time. Recall that J denotes the index set (m, j, l), and $\hat{H}_J$ and Z_l are horizontal and vertical structure functions, respectively. All the notations are defined in Part I to which the reader is referred for the appropriate definitions.

The horizontal velocity can be decomposed into a nondivergent part, $\mathbf{k} \times \nabla\psi$, and a divergent part $\nabla\chi$. Thus, the kinetic energy of the whole atmosphere is given by

$$K = K_\chi + K_\psi, \quad (3)$$

where

$$K_\chi = \frac{1}{2} \int \nabla\chi \cdot \nabla\chi dM, \quad (4)$$

$$K_\chi = \frac{1}{2}\int (\mathbf{k}\times\nabla\psi)\cdot(\mathbf{k}\times\nabla\psi)dM, \quad (5)$$

$$\int (\ )dM = \frac{a^2}{g}\int_{-1}^{1}\int_0^{2\pi}\int_0^1 (\ )p_s d\sigma d\lambda d\mu. \quad (6)$$

Here dM is an element of mass of the atmosphere, and K_χ and K_ψ are the divergent and nondivergent kinetic energy, respectively.

We define the available potential energy $\tilde{P}$ as

$$\tilde{P} = \frac{1}{2}\int\left[\frac{\sigma}{R\Gamma_0}\left(\frac{\partial\hat{\phi}}{\partial\sigma}\right)^2 + \tilde{P}_s\right]dM, \quad (7)$$

where the subscript s denotes the surface value, and

$$\tilde{P}_s = \frac{T_{0s}}{R\Gamma_{0s}^2}\left(\frac{\partial\hat{\phi}}{\partial\sigma}\right)_s^2. \quad (8)$$

The term $\tilde{P}_s$ is introduced so that the surface contribution to the available potential energy is taken into account. Note that this form has not been used previously. However, this term is consistent with the boundary conditions used in deriving and solving the vertical structure equation in Kasahara and Puri (1981). This definition not only leads to a "neat" formulation of energy relations later but also *conserves* the total energy of the *linearized* system, which is defined as

$$E = K_\chi + K_\psi + \tilde{P}. \quad (9)$$

Substituting (1) into (3)–(7), using the boundary conditions, and applying the vertical structure equation (Ko 1985), the total energy (9) can be written as

$$E = \frac{1}{2}\int\sum_{J,J'}[(\hat{\tilde{P}})_{J,J'} + (\hat{K}_\psi)_{J,J'} + (\hat{K}_\chi)_{J,J'}] \times \alpha_J\alpha_{J'}^* Z_l Z_{l'} dM, \quad (10)$$

where

$$(\hat{\tilde{P}})_{J,J'} = \frac{\hat{\Phi}_J\hat{\Phi}_{J'}^*}{gD_l}, \quad (11)$$

$$(\hat{K}_\psi)_{J,J'} = -\hat{\Psi}_J\nabla^2\hat{\Psi}_{J'}^*, \quad (12)$$

$$(\hat{K}_\chi)_{J,J'} = -\hat{X}_J\nabla^2\hat{X}_{J'}^*. \quad (13)$$

Since the vertical structure functions as well as horizontal modes are orthogonal to each other, the general expression for the total energy (10) can further be simplified. Using the orthogonality conditions of vertical and horizontal structure functions, (10) becomes

$$E = \frac{1}{2}\int\sum_J[(\hat{\tilde{P}})_J + (\hat{K}_\psi)_J + (\hat{K}_\chi)_J]\alpha_J\alpha_J^* dA, \quad (14)$$

where

$$(\hat{\tilde{P}})_J = \frac{\hat{\Phi}_J\hat{\Phi}_J^*}{gD_l}, \quad (15)$$

$$(\hat{K}_\psi)_J = -\hat{\Psi}_J\nabla^2\hat{\Psi}_J^*, \quad (16)$$

$$(\hat{K}_\chi)_J = -\hat{X}_J\nabla^2\hat{X}_J^*, \quad (17)$$

$$\int (\ )dA = \frac{a^2}{g}\int_{-1}^{1}\int_0^{2\pi} (\ )p_s d\lambda d\mu. \quad (18)$$

Since the surface pressure p_s in (18) is a function of longitude and latitude, (14) must be integrated through the whole horizontal domain. With some loss of generality, the surface pressure is approximated by the horizontally averaged surface value $\bar{p}_s$ and (14) is further simplified. After using the orthogonality condition of horizontal modes, the energy expression (14) thus becomes

$$E = \frac{\pi a^2\bar{p}_s}{g}\sum_J E_J, \quad (19)$$

where

$$E_J = \alpha_J\alpha_J^*. \quad (20)$$

Equations (19) and (20) demonstrate that the total energy can be represented by the modal amplitudes of the horizontal modes for each vertical mode. The energy can therefore be separated into the contributions from the rotational and gravitational modes.

3. Zonal energy and meridional energy

The nondivergent part of horizontal velocity is related to the strength of vorticity and the divergent part measures the strength of the divergence field. To examine the effect of the gravitational modes on the divergence field, it is useful to investigate the distributions of the velocity potential χ, which provides information on the vertical circulation. If the isopleths of the velocity potential χ are parallel to the meridians, then there would be no meridional circulation. If the isopleths of the velocity potential are parallel to latitude circles, then the divergent east–west (or zonal) circulation would be missing. Similarly, if the isopleths of the streamfunction ψ are parallel to the meridians, there would be no nondivergent zonal motion. If the isopleths of the streamfunction are parallel to the latitude circles, the nondivergent meridional motion would be missing. These arguments suggest that more information about the circulations and vorticity can be drawn if both the divergent and nondivergent velocities are split into zonal and meridional components. The zonal and meridional components of the divergent (or nondivergent) kinetic energy can be obtained from the zonal and meridional component of the divergent (or nondivergent) part of the velocity field. Consequently, the kinetic energy of the whole atmosphere can be expressed as

$$K = K_{\chi\lambda} + K_{\chi\mu} + K_{\psi\lambda} + K_{\psi\mu}, \quad (21)$$

where

$$K_{\chi\lambda} = \frac{1}{2a^2}\int \frac{1}{(1-\mu^2)}\left[\frac{\partial\chi}{\partial\lambda}\right]^2 dM, \quad (22)$$

$$K_{\chi\mu} = \frac{1}{2a^2}\int (1-\mu^2)\left[\frac{\partial\chi}{\partial\mu}\right]^2 dM, \quad (23)$$

$$K_{\psi\lambda} = \frac{1}{2a^2}\int (1-\mu^2)\left[\frac{\partial\psi}{\partial\mu}\right]^2 dM, \quad (24)$$

$$K_{\psi\mu} = \frac{1}{2a^2}\int \frac{1}{(1-\mu^2)}\left[\frac{\partial\psi}{\partial\lambda}\right]^2 dM. \quad (25)$$

Here $K_{\chi\lambda}$ and $K_{\chi\mu}$ are the zonal and meridional components of K_χ, respectively, and $K_{\psi\lambda}$ and $K_{\psi\mu}$ are the zonal and meridional components of K_ψ, respectively. The $K_{\chi\lambda}$ and $K_{\chi\mu}$ measure the strengths of the divergent *zonal* and *meridional* circulations, respectively; whereas, $K_{\psi\lambda}$ and $K_{\psi\mu}$ estimate the strength of nondivergent zonal and meridional motions, respectively. This form of energy decomposition, (21), has not been previously used.

It follows from (1) and (22)–(25) that the zonal and meridional components of the divergent and nondivergent kinetic energy can be expressed as

$$\begin{pmatrix} K_{\chi\lambda} \\ K_{\psi\mu} \end{pmatrix} = \frac{1}{2a^2} \times \int \left\{ \frac{1}{1-\mu^2}\left[\sum_J \alpha_J \alpha_J^* \frac{\partial}{\partial\lambda}\begin{pmatrix} \hat{X}_J \\ \hat{\Psi}_J \end{pmatrix} \frac{\partial}{\partial\lambda}\begin{pmatrix} \hat{X}_J^* \\ \hat{\psi}_J^* \end{pmatrix} \right] \right\} dA \quad (26)$$

$$\begin{pmatrix} K_{\chi\mu} \\ K_{\psi\lambda} \end{pmatrix} = \frac{1}{2a^2} \times \int \left\{ (1-\mu^2)\left[\sum_J \alpha_J \alpha_J^* \frac{\partial}{\partial\mu}\begin{pmatrix} \hat{X}_J \\ \hat{\Psi}_J \end{pmatrix} \frac{\partial}{\partial\mu}\begin{pmatrix} \hat{X}_J^* \\ \hat{\Psi}_J^* \end{pmatrix} \right] \right\} dA. \quad (27)$$

Equations (26) and (27) can further be expressed in terms of spherical harmonics and modal amplitudes associated with different vertical modes.

4. Numerical results and discussions

To investigate the energetics, we use two historical datasets from 1200-day perpetual January simulations with the CCM0B (Williamson 1983). The simulations were made using a 30-minute time step and sampled every 12 h. The first and second datasets consist of days 60–74.5 and 210–224.5, respectively. There are 30 files (15 days) in each dataset. The choice of dataset is arbitrary. Time averages are computed over all 60 files. The rotational and gravitational energy can be obtained by integrations of (14)–(18) and (26)–(27) via Gaussian quadrature (Machenhauer 1979).

In order to compare the *relative* importance of energy components, all the components of gravitational (or rotational) energy are normalized by total global gravitational (or global rotational) energy. One advantage for using normalized values instead of absolute ones is that the results may be more independent of data length. Note that we used percentage instead of ratio itself to amplify the magnitude of results.

a. Classification of eigenfrequencies

In this study, we use rhomboidal-15 truncation, i.e., 16 zonal wavenumbers (m) and 16 meridional modes (n). For each set (m, n, l), there are three eigenfrequencies of which one is westward gravity wave, one eastward gravity wave, and one Rossby wave. Because the total number of eigenfrequencies is quite large ($6912 = 3 \times 16 \times 16 \times 9$), they will be grouped according to the meridional modes n affiliated with each vertical mode l. The meridional index (I) will be used to denote the frequency category corresponding to each vertical mode for all zonal wavenumbers and every two successive n's ($n - |m| = 2I - 1, 2I$). Therefore, for each vertical mode, meridional index 1 is associated with the first and second n's ($n - |m| = 1, 2$) and zonal wavenumbers 0–15, index 2 with the third and fourth n's ($n - |m| = 3, 4$) and zonal wavenumbers 0–15, and so forth. Because there are 16 meridional modes n, the frequencies are classified into eight categories for either westward or eastward gravity waves, and eight for Rossby waves. Note that, for each zonal wavenumber and each meridional index, the higher the vertical mode the lower the gravity- and Rossby-wave frequencies. For each zonal wavenumber and each vertical mode, the higher the meridional index the higher the gravity-wave frequency but the lower the Rossby-wave frequency. For each meridional index and each vertical mode below 5, the higher the zonal wavenumber the higher the gravity-wave frequency.

b. Rotational energy among meridional indices, vertical modes, and zonal waves

The rotational component of the kinetic energy K_r among meridional indices (I), vertical modes (l), and zonal wavenumber (m) is illustrated in Fig. 2. It is clear that K_r is concentrated in lower vertical modes 0–4, meridional indices 2–5, and zonal wavenumbers 1–8. Vertical mode 1 with index 3 and wavenumber 3 plays the most important role in K_r. But planetary waves related to vertical modes 3–4 are also important. In general, shorter waves contribute smaller rotational kinetic energy.

Contributions to rotational component of the available potential energy (Fig. 3) are mainly from vertical modes 3–5, meridional indices lower than 3, and zonal wavenumbers 1–3. Recall that for each vertical mode, the higher the meridional index the lower the Rossby-wave frequency. This implies that for each vertical mode, the Rossby waves with lower frequencies (I

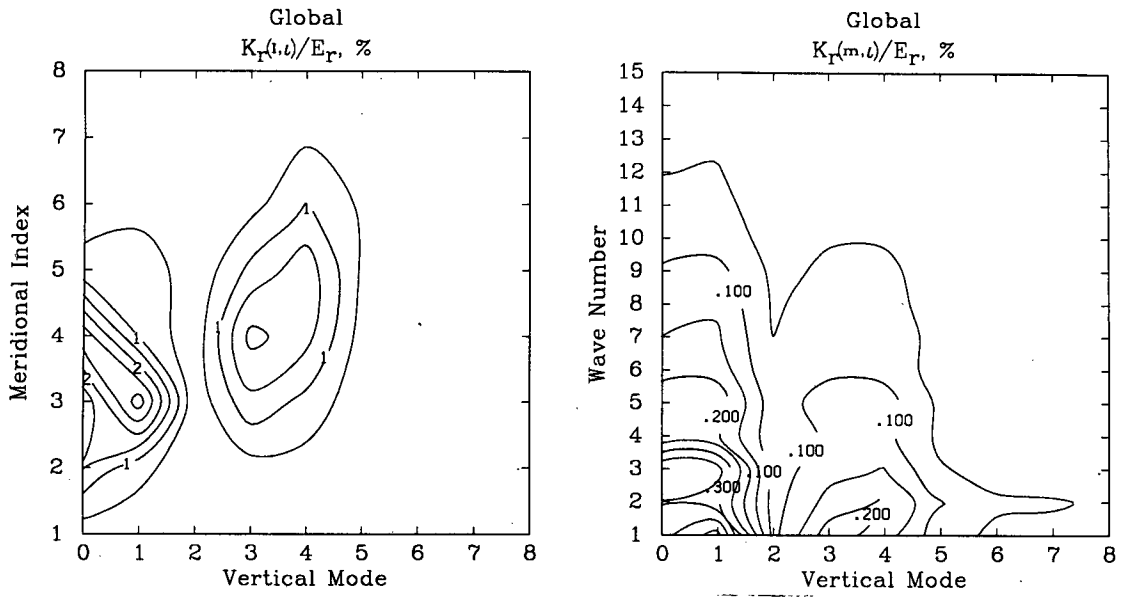

FIG. 2. Distributions of rotational kinetic energy among meridional indices (I), vertical modes (l), and zonal wavenumbers (m) with respect to the total global rotational energy E_r. (a) $K_r(I, l)$, the contour interval is 0.5%; (b) $K_r(m, l)$, the contour interval is 0.05%.

> 3) do not contribute much to the rotational available potential energy. Vertical mode 4 with index 2 contributes the most to $\tilde{P}_r(I, l)$. However, in contrast to K_r, the contributions of vertical modes 0–2 to $\tilde{P}_r$ are negligible. The local maximum for $\tilde{P}_r$ around vertical mode 8, which is a consequence of dividing by small equivalent depth, might not be reliable.

Note that the values of $K_r(I, l)$ and $\tilde{P}_r(I, l)$ are much larger than those of $K_r(m, l)$ and $\tilde{P}_r(m, l)$, respectively. The reasons are that for each vertical mode the rotational energy is distributed much more extensively among zonal waves than among meridional indices and that there are 16 zonal wavenumbers but only 8 meridional indices.

It follows that in the vertical mode range 3–5 the rotational available potential energy dominates, while

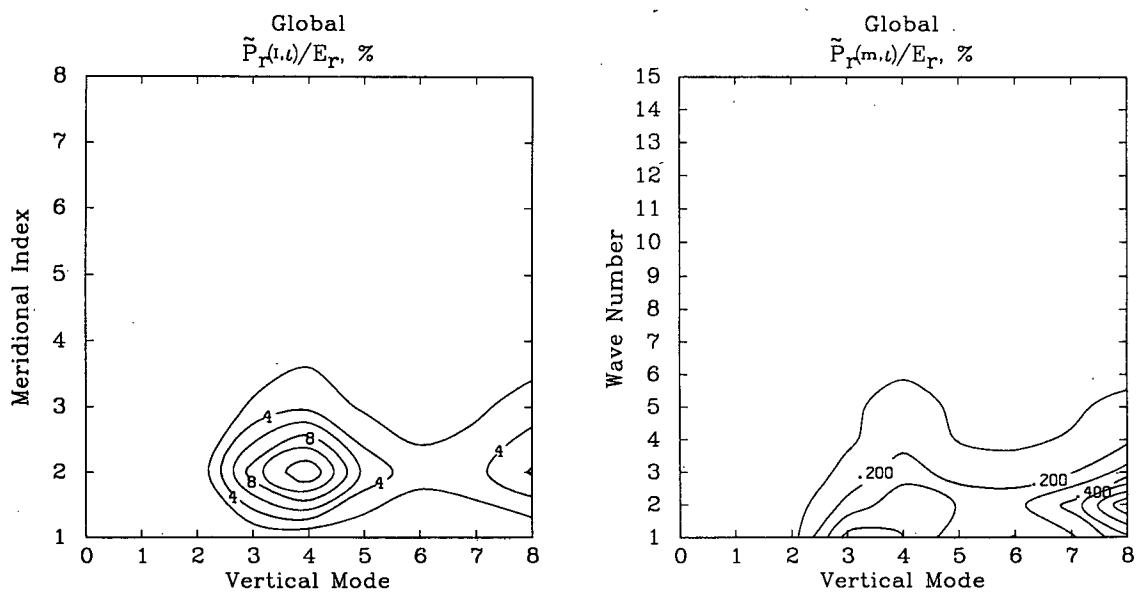

FIG. 3. Distributions of rotational available potential energy among meridional indices (I), vertical modes (l), and zonal wavenumbers (m) with respect to the total global rotational energy E_r. (a) $\tilde{P}_r(I, l)$, the contour interval is 2%; (b) $\tilde{P}_r(m, l)$, the contour interval is 0.1%.

the rotational kinetic energy governs in the lower vertical modes 0–4. In general, the rotational available potential energy is much larger than the rotational kinetic energy in the global region. This is consistent with Lorenz's (1967) results. Because K_r dominates in lower vertical modes and $\tilde{P}_r$ dominates in relatively higher vertical modes, the total rotational energy E_r, which is the sum of K_r and $\tilde{P}_r$, is distributed extensively in the global region among vertical modes 0–5.

c. *Gravitational energy among meridional indices, vertical modes, and zonal waves*

1) AVAILABLE POTENTIAL ENERGY

Figure 4 shows the percentage distributions among meridional indices (I), vertical modes (l), and zonal wavenumbers (m) for the gravitational component of available potential energy $\tilde{P}_g$ with respect to the total global gravity energy. $\tilde{P}_g(I, l)$ is confined within a small region between modes 1 and 6, below meridional index 2. For $\tilde{P}_g(m, l)$, vertical mode 3 dominates through most zonal wavenumbers. Wavenumbers 1–5 with vertical modes 1–4 contribute most of the available potential energy.

Thus the gravitational available potential energy is contributed mainly by vertical modes 1–5, meridional indices 1–2, and zonal wavenumbers 1–5. This implies that short gravity waves are not so important to the available potential energy. In fact, the gravitational available potential energy is smaller than the corresponding gravitational kinetic energy. Thus, some gravitational kinetic energy may be created by conversion from rotational available potential energy.

2) DIVERGENT AND NONDIVERGENT KINETIC ENERGY

It is obvious from Fig. 5a that the distribution of divergent kinetic energy $K_{\chi g}(I, l)$ is concentrated near medium vertical modes 2–5 and lower meridional indices 1–3. $K_{\chi g}(m, l)$ is due mostly to planetary and intermediate waves 1–10 associated with vertical modes 2–6 (Fig. 5b). Nevertheless, the contributions of short waves related to modes 2–6 are not negligible. Vertical mode 3 dominates at the planetary scale, but for smaller scales, modes 4 and 5 contribute the most. Vertical modes 0 and 1 contribute little in all zonal wavenumbers.

The distribution of the nondivergent kinetic energy is shown in Fig. 6. It is clear that the distribution of $K_{\psi g}(I, l)$ is more extensive than $K_{\chi g}(I, l)$ and is spread over vertical modes 2–7 and meridional indices 1–7. But for $K_{\psi g}(m, l)$, only the planetary and synoptic waves 1–7 associated with vertical modes 2–6 are important. Consequently, short gravity waves are more important for the divergent kinetic energy than for the nondivergent one.

From Figs. 5–6, it is evident that the divergent kinetic energy is much more important than the nondivergent energy in contributions to the global gravitational energy. Contributions to the divergent kinetic energy are mostly from vertical modes 2–6, meridional indices 1–3, and zonal wavenumbers 1–10. For the nondivergent kinetic energy, vertical modes 2–6, meridional indices 1–7, and zonal wavenumbers 1–7 are important. Gravity waves with large meridional indices ($I > 3$) do not contribute much to the divergent kinetic energy

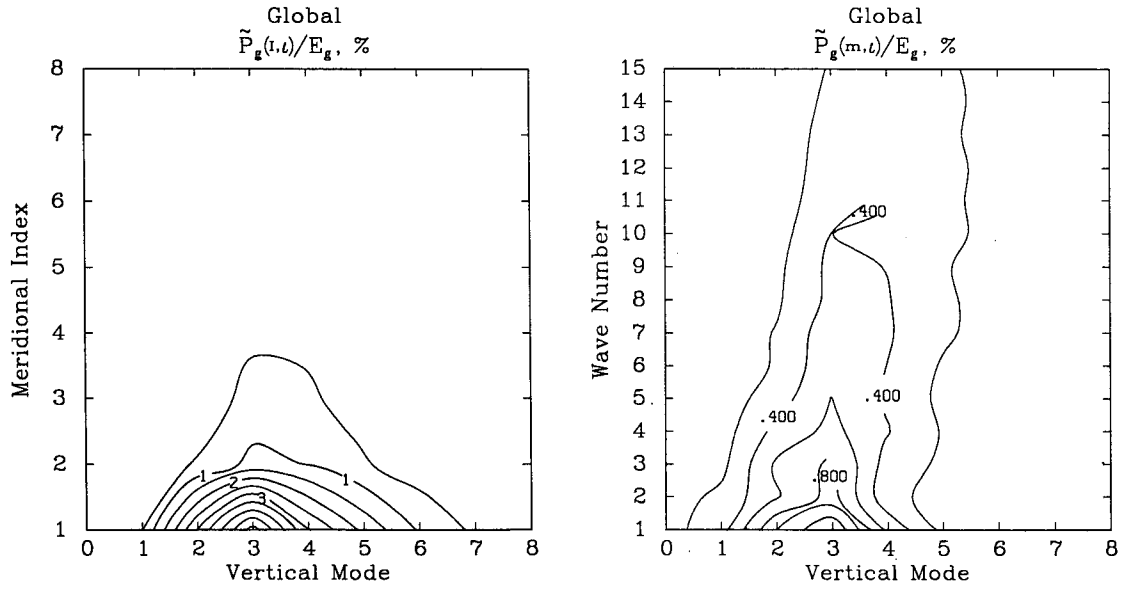

FIG. 4. Distributions of gravitational component of available potential energy among meridional indices (I), vertical modes (l), and zonal wavenumbers (m) with respect to the total global gravity energy E_g. (a) $\tilde{P}_g(I, l)$, the contour interval is 0.5%; (b) $\tilde{P}_g(m, l)$, the contour interval is 0.2%.

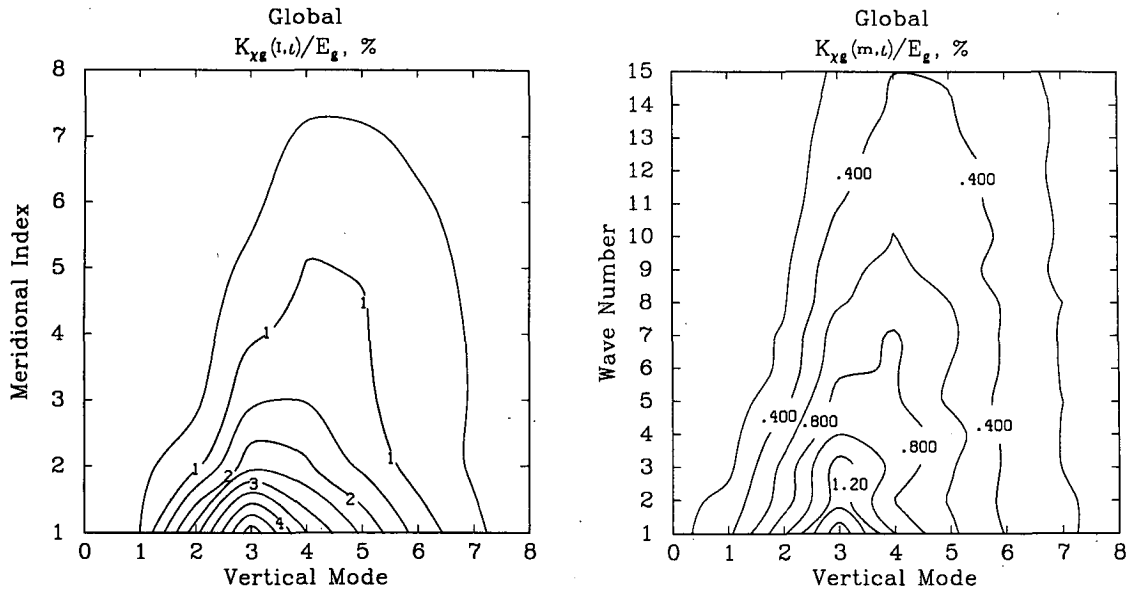

FIG. 5. Distributions of gravitational divergent kinetic energy among meridional indices (I), vertical modes (l), and zonal wavenumbers (m) with respect to the total global gravity energy E_g. (a) $K_{\chi g}(I, l)$, the contour interval is 0.5%; (b) $K_{\chi g}(m, l)$, the contour interval is 0.2%.

and short zonal waves ($m > 7$) are not important to the nondivergent kinetic energy.

3) ZONAL AND MERIDIONAL COMPONENTS OF DIVERGENT KINETIC ENERGY

Figure 7 illustrates the distributions of the zonal components of divergent kinetic energy $K_{\chi g}$ among meridional indices, vertical modes, and zonal wavenumbers with respect to their total sum instead of total gravity energy. Figure 7a shows that vertical modes 2–6 with meridional indices 1–3 dominate the zonal component $K_{\chi\lambda g}(I, l)$ and that the contributions of vertical modes 0, 1 and 8 for all indices are negligible. Figure 7b shows that the main contributions to $K_{\chi\lambda g}(m, l)$ are from vertical modes 2–6 and zonal wavenumbers

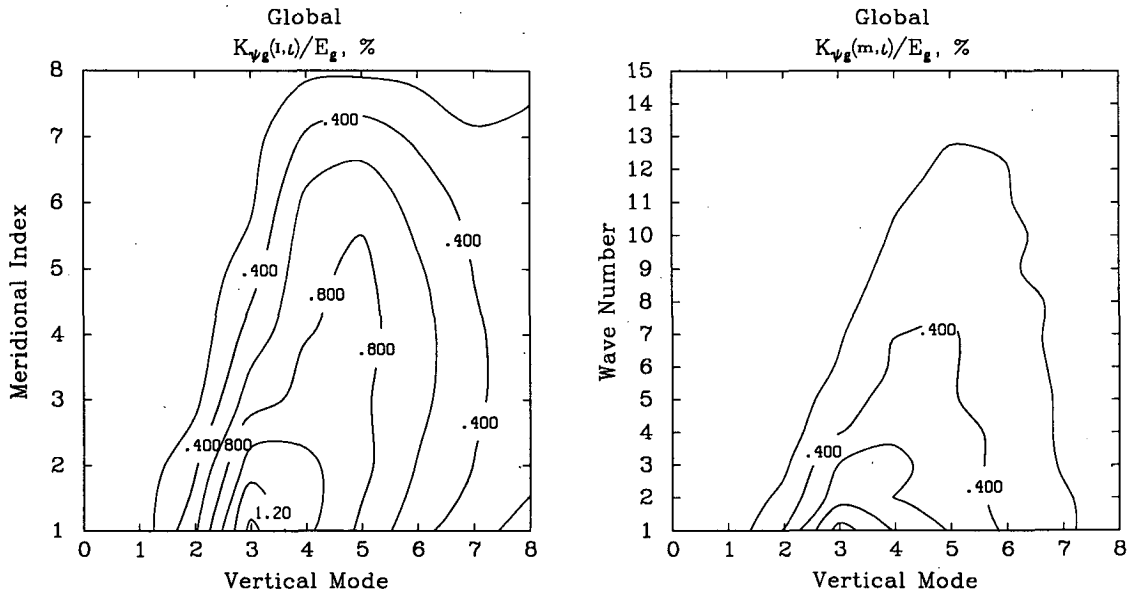

FIG. 6. Distributions of gravitational nondivergent kinetic energy among meridional indices (I), vertical modes (l), and zonal wavenumbers (m) with respect to the total global gravity energy E_g. (a) $K_{\psi g}(I, l)$, the contour interval is 0.2%; (b) $K_{\psi g}(m, l)$, the contour interval is 0.2%.

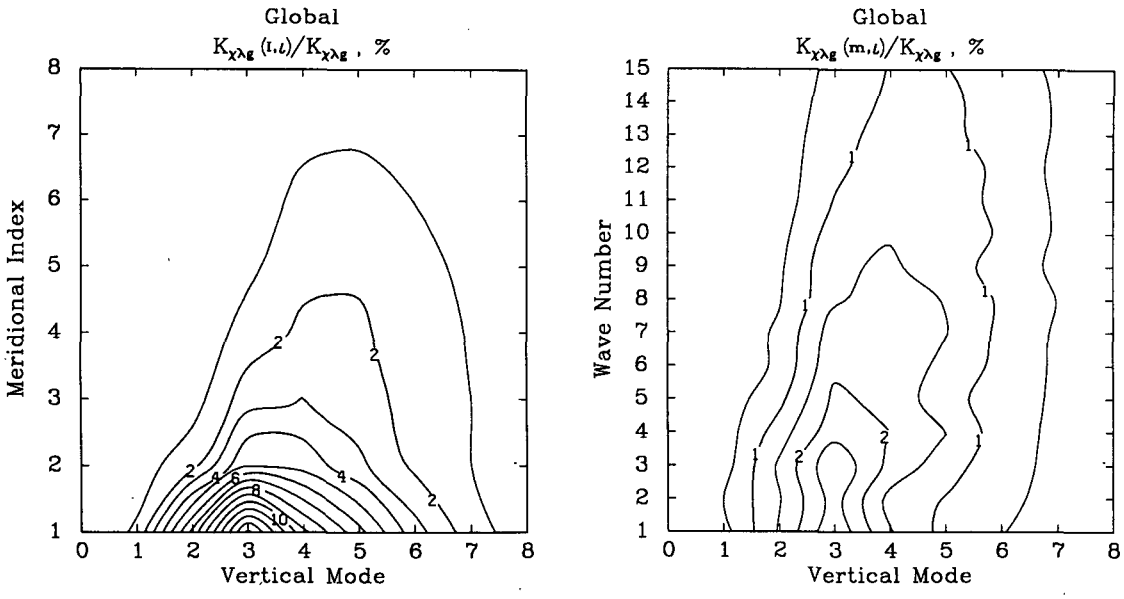

FIG. 7. Distributions of the zonal component of gravitational divergent kinetic energy among meridional indices (I), vertical modes (l), and zonal wavenumbers (m) with respect to their total sum in the global region. (a) $K_{\chi\lambda g}(I, l)$, the contour interval is 1%; (b) $K_{\chi\lambda g}(m, l)$, the contour interval is 0.5%.

1–10, while the contributions from vertical modes 0, 1, 7 and 8 are negligible. Vertical mode 3 for zonal wavenumbers 1–5 contributes the most to the zonal component.

From the above statements we conclude that the gravity waves associated with vertical modes 2–6, meridional indices below 4, and zonal wavenumbers below 10 are responsible for the global divergent east–west circulation. However, all gravity waves associated with vertical modes 0, 1, 7 and 8 can be adjusted or removed initially without seriously affecting the divergent east–west circulation. Here we have assumed that the time tendencies of gravity waves which contribute little to the long-term averaged energy contents of the divergent circulations should be small initially.

Compared to zonal energy, the meridional energy $K_{\chi\mu g}(I, l)$ (Fig. 8a) is distributed more evenly between vertical modes 2 and 6 and between meridional indices 1 and 7. The contributions of zonal waves to $K_{\chi\mu g}(m, l)$ (Fig. 8b) decrease with zonal wavenumbers more rapidly than those for $K_{\chi\lambda g}(m, l)$. Apparently, modes 2–6 with wavenumbers 1–10 contribute significantly to the meridional circulation. It is obvious that wavenumbers above 10 for all vertical modes do not contribute much to the meridional circulation.

Therefore, the gravity waves associated with vertical modes 2–6, meridional indices below 7, and zonal wavenumbers 1–10 are mainly responsible for the global meridional circulation. But the gravity waves associated with vertical modes 0, 1, 7 and 8 can be freely adjusted without seriously weakening the strength of the global meridional circulation. Note that the zonal circulation is stronger than the meridional one and the higher meridional indices, 4–7, are much more important for meridional circulation than for zonal circulation.

The above results explain why the scheme of Puri and Bourke (1982) can retain the Hadley circulation. The main reason is that, in their scheme, the important gravity waves related to vertical modes 2–6 with frequencies less than the cutoff frequency are not adjusted. Their cutoff frequency is defined as the lowest frequency corresponding to the first internal mode for each zonal wavenumber. This cutoff frequency is equivalent to that frequency, in our case, associated with the first internal mode, the first meridional index, and zonal wavenumber 1. As mentioned previously, the higher the meridional index the higher the gravity-wave frequency for fixed vertical mode and zonal wavenumber, and the higher the zonal wavenumber the higher the gravity-wave frequency for each meridional index and each vertical mode below 5. For example, the frequency of an important gravity wave with vertical mode 3, zonal wavenumber 2, and meridional index 2 is higher than the cutoff frequency. This means that some important gravity waves with frequencies higher than their cutoff frequency are adjusted during the initialization and thus the large-scale circulations may be distorted. Similar arguments can be applied to explain why the spinup time for the initialized data from Kitade's scheme is much larger than that for the analysis data.

Consequently, to adjust the gravity waves in the initialization based only on the cutoff frequency or vertical modes may not be proper and may distort the divergence field, which depends not only on frequency or

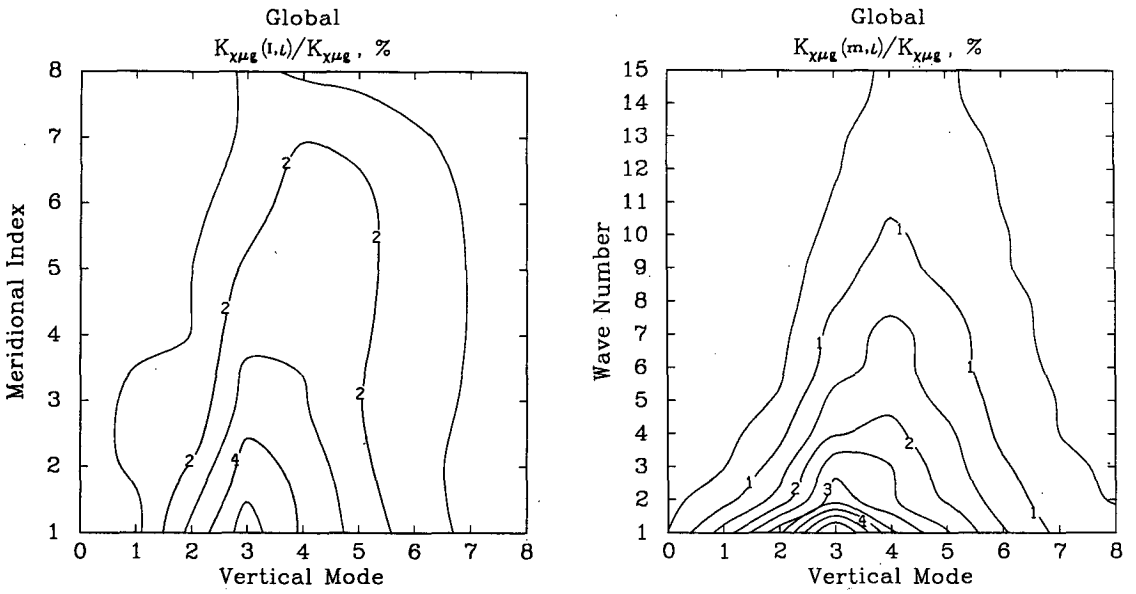

FIG. 8. Distributions of the merdional component of gravitational divergent kinetic energy among meridional indices (I), vertical modes (l), and zonal wavenumbers (m) with respect to their total sum in the global region. (a) $K_{\chi\mu g}(I, l)$, the contour interval is 1%; (b) $K_{\chi\mu g}(m, l)$, the contour interval is 0.5%.

vertical mode. It is more appropriate to adjust gravity waves based on vertical modes, meridional indices, and zonal wavenumbers.

4) ZONAL AND MERIDIONAL COMPONENTS OF NONDIVERGENT KINETIC ENERGY

The parameter $K_{\psi\lambda g}$ represents the zonal component of gravitational nondivergent kinetic energy. From Fig. 9, we note that the contribution of zonal nondivergent kinetic energy is mainly due to vertical modes 2–6, meridional indices 1–7, and zonal wavenumbers 1–8. This means that the external and first internal modes contribute little to $K_{\psi\lambda g}$ and that short waves ($m > 8$) are not very important. The $K_{\psi\lambda g}$ peaks at wavenumber 1, vertical mode 3, and meridional index 2.

The meridional component of gravitational nondi-

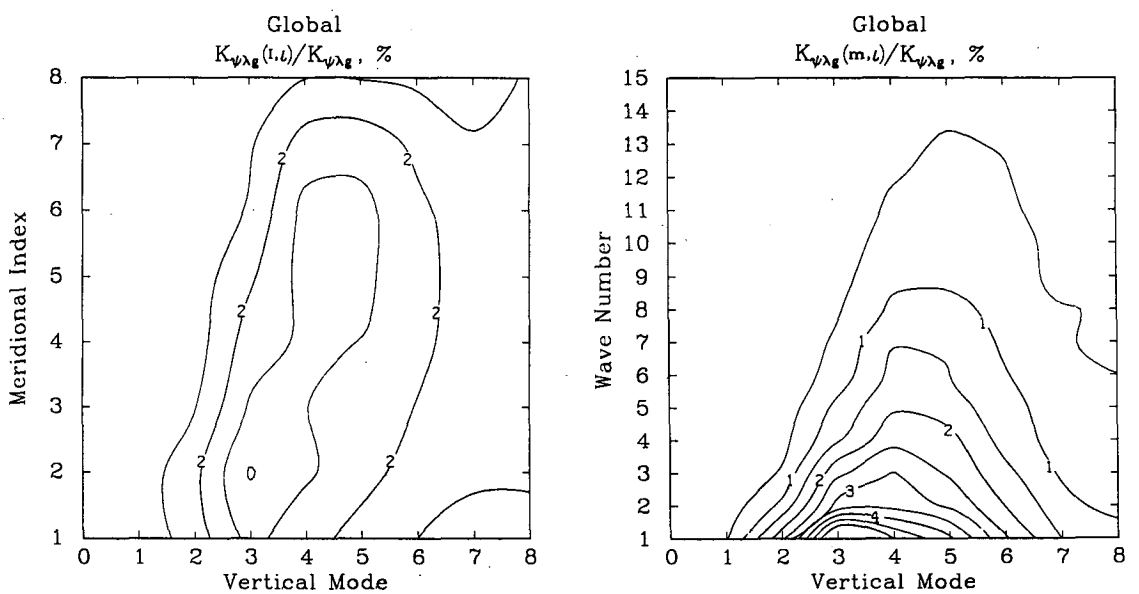

FIG. 9. Distributions of the zonal component of gravitational nondivergent kinetic energy among meridional indices (I), vertical modes (l), and zonal wavenumbers (m) with respect to their total sum in the global region. (a) $K_{\psi\lambda g}(I, l)$, the contour interval is 1%; (b) $K_{\psi\lambda g}(m, l)$, the contour interval is 0.5%.

vergent kinetic energy is shown in Fig. 10. We see that the major contributions to $K_{\psi\mu g}$ are mostly from vertical modes 2–6, meridional indices 1–6, and zonal wavenumbers 1–12. Similarly, all gravity waves associated with modes 0 and 1 are negligible in the $K_{\psi\mu g}$.

By comparing Figs. 9 and 10, we find that the zonal nondivergent kinetic energy is comparable to the meridional nondivergent kinetic energy, although the former is slightly smaller. However, short waves ($m > 8$) are more important for meridional nondivergent kinetic energy than for zonal nondivergent kinetic energy.

Therefore, gravity waves associated with vertical modes 2–6, meridional indices 1–7, and zonal wavenumbers 1–12 are important in nondivergent kinetic energy. Our results indicate that the distributions of divergent and nondivergent kinetic energies are concentrated in the similar ranges among vertical modes, meridional indices, and zonal waves. Thus, inappropriate adjustment of gravity waves in the initialization may weaken both vorticity and divergence, distort the synoptic scale pressure systems, and cause the spinup problem.

5. Summary and concluding remarks

A new approach to energetics is used to investigate the global east–west and meridional circulations. All the energy components are separated into gravitational and rotational parts. In particular, the *gravitational* divergent kinetic energy is split into *zonal* and *meridional* components which measure the strength of the east–west and meridional circulations, respectively. The zonal and meridional components of gravitational nondivergent kinetic energy are examined. We also introduce a new, easy and reasonable criterion to adjust the gravity waves during the initialization based on vertical modes, meridional indices, and zonal wavenumbers rather than frequency and/or vertical modes only. This approach can not only *retain the large-scale circulations* but also *preserve the synoptic scale pressure systems*. Note that this technique can be applied to other forecasting models although the numerical values might not be the same for different models.

The rotational part of the global available potential energy is more than twice as much as the rotational part of the global nondivergent kinetic energy. The majority of the rotational available potential energy resides in higher vertical modes 3–5, lower meridional indices 0–2, and lower zonal wavenumbers 1–3, while the majority of the rotational kinetic energy resides in lower vertical modes 0–4, intermediate meridional indices 2–5, and zonal wavenumbers below 9.

Contributions to the global east–west circulation are mostly from vertical modes 2–6, meridional indices 1–5 and zonal wavenumbers 1–10. Note that the third internal mode corresponding to wavenumber 1 and meridional index 1 plays the most important role in the global zonal circulation.

The divergent kinetic energy of the global meridional circulation resides primarily in vertical modes 2–6 with meridional indices 1–6 and zonal waves 1–10. Note that the third internal mode related to the longest zonal waves and first meridional index contribute the most to the meridional circulation. However, all the gravity

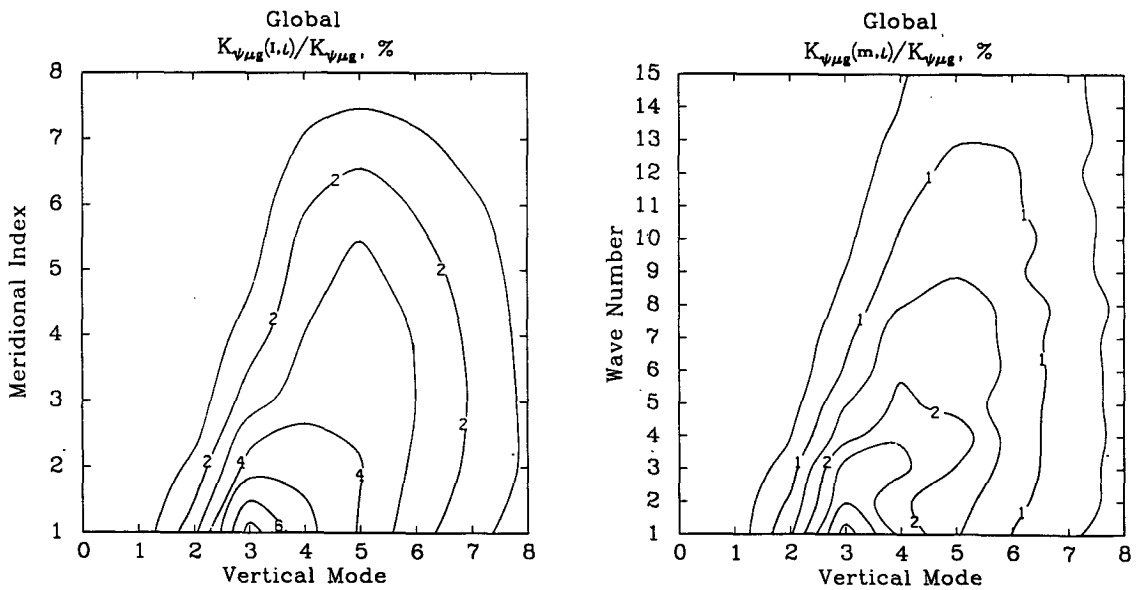

FIG. 10. Distributions of the meridional component of gravitational nondivergent kinetic energy among meridional indices (I), vertical modes (l), and zonal wavenumbers (m) with respect to their total sum in the global region. (a) $K_{\psi\mu g}(I, l)$, the contour interval is 1%; (b) $K_{\psi\mu g}(m, l)$, the contour interval is 0.5%.

waves associated with the external and the first internal modes contribute little to the meridional circulation.

Globally, the contribution of the zonal component of nondivergent kinetic energy is slightly smaller than that of the meridional component. Contributions to both zonal and meridional components of the nondivergent kinetic energy are mainly from vertical modes 3–6 and meridional indices 1–7. However, shorter waves ($m > 9$) are not as important for the meridional component as for the zonal component.

Based on the above results we recommend that the gravity waves corresponding to the internal modes 2–6 associated with zonal wavenumbers 1–10 and meridional indices 1–6 not be adjusted signficantly in the initialization in order to retain the strength of both zonal and meridional circulations and of the vorticity which is important in maintaining the synoptic scale pressure systems. The gravity waves corresponding to internal modes 2–6 associated with zonal wavenumbers larger than 10 and meridional indices larger than 6 can be adjusted in the initialization. Particularly, all gravity waves associated with the external and the first internal modes can be adjusted freely in the initialization to reduce high-frequency oscillations. To adjust the gravity waves based only on frequency or vertical mode might distort substantially the divergence and vorticity fields and thus might cause a spinup problem.

The conclusions of this study are based on the perpetual January data of NCAR Community Climate Model, which has fairly coarse resolution. We expect that the effects of a substantial change of resolution or physics on the energy distributions may be significant for some small scales in the model. There may be modes in the real atmosphere, such as relatively large-scale convective systems, which the model may not simulate properly. It may be important to retain these modes in the initial conditions, especially for short to medium range forecasts. To confirm this, a similar energetics analysis of real data is necessary.

Acknowledgments. This work is based in small part on the Ph.D. dissertation of Shun Der Ko. Support for this research was provided by NCAR and The University of Michigan. This work was partially supported by NSF Grant OCE 8305648. We are grateful to Dr. Ron Errico for providing his initialization software and to Dr. Akira Kasahara for his helpful suggestions. The comments of anonymous reviewers led to substantial improvements in the manuscript.

REFERENCES

Baer, F., 1977: Adjustment of initial conditions required to suppress gravity oscillations in non-linear flows. *Beitr. Phys. Atmos.*, **50,** 350–366.

Burrows, W. R., 1976: A diagnostic study of atmospheric spectral kinetic energetics. *J. Atmos. Sci.*, **33,** 2308–2321.

Chen, T. C., and A. Wiin-Nielsen, 1976: On the kinetic energy of the divergent and nondivergent flow in the atmosphere. *Tellus,* **28,** 486–497.

Kasahara, A., and K. Puri, 1981: Spectral representation of three-dimensional global data by expansion in normal mode functions. *Mon. Wea. Rev.*, **109,** 37–51.

Kitade, T., 1983: Nonlinear normal mode initialization with physics. *Mon. Wea. Rev.*, **111,** 2194–2213.

Ko, S. D., 1985: Vertical modes and energetics of gravitational and rotational modes in a multilevel global spectral model. Ph.D. dissertation, The University of Michigan, 225 pp. [Available as NCAR Cooporative Thesis NCAR/CT-95, National Center for Atmospheric Research, Boulder, CO 80307.]

——, J. Tribbia and J. Boyd, 1989: Energetics analysis of a multilevel global spectral model. Part I: Balanced energy and transient energy. *Mon. Wea. Rev.*, **117,** 1941–1953.

Lorenz, E. N., 1967: *The Nature and Theory of the General Circulation of the Atmosphere.* World Meteor. Org., 161 pp.

Machenhauer, B., 1977: On the dynamics of gravity oscillations in a shallow water model, with application to nonlinear normal mode initialization. *Beitr. Phys. Atmos.*, **50,** 253–271.

——, 1979: The spectral method. *Numerical Methods Used in Atmospheric Models. GARP Publ. Ser.*, **17,** 121–275.

Puri, K., and W. Bourke, 1982: A scheme to retain the Hadley circulation during nonlinear normal mode initialization. *Mon. Wea. Rev.*, **110,** 327–335.

Williamson, D. L., 1983: Description of NCAR Community Climate Model, NCAR Tech. Note, NCAR/TN-210+STR, 88 pp. [NTIS No. PB83-231068.]